

Pure Luminosity Evolution models for faint field galaxy samples

L. Pozzetti^{1,2}, G. Bruzual A.^{3,4}, and G. Zamorani^{2,5}

¹*Dipartimento di Astronomia, Università di Bologna, via Zamboni 33, I-40126 Bologna, Italy (lucia@astbo3.bo.astro.it)*

²*Osservatorio Astronomico di Bologna, via Zamboni 33, I-40126 Bologna, Italy (zamorani@astbo3.bo.astro.it)*

³*Centro de Investigaciones de Astronomía, A.P. 264, Mérida 5101-A, Venezuela (bruzual@cida.ve)*

⁴*Landessternwarte Heidelberg Königstuhl, D-69117 Heidelberg, Germany*

⁵*Istituto di Radioastronomia del CNR, via Gobetti 101, I-40129 Bologna, Italy*

Accepted April 1996

ABSTRACT

We have examined a set of pure luminosity evolution (PLE) models in order to explore up to what extent the rapidly increasing observational constraints from faint galaxy samples can be understood in this simple framework. We find that a PLE model, in which galaxies evolve mildly in time even in the rest frame UV, can reproduce most of the observed properties of faint galaxies assuming an open ($\Omega \sim 0$) universe. In particular, such a model is able to fit reasonably well the number counts in the U , b_j , r_f , I , and K bands, as well as the colour and redshift distributions derived from most of the existing samples. The most significant discrepancy between the predictions of this model and the data is the z distribution of faint K -selected galaxies. Significantly worse fits are obtained with PLE models for the theoretically attractive value of $\Omega = 1$, although a simple number luminosity evolution model with a significant amount of merger events fits the data also in this cosmology.

Key words: galaxies: evolution - galaxies: photometry - galaxies: redshifts - cosmology: miscellaneous.

1 INTRODUCTION

An impressively large amount of observations of faint field galaxies has been collected over the last fifteen years. The determination of galaxy number counts, colour and redshift (z) distributions of increasingly deep samples is now part of the observational routine of several established groups. Since the review paper by Koo & Kron (1992), galaxy photometric surveys have been extended to $b_j = 27.5$ (Metcalfe et al. 1995a) and to $K < 24$ (Gardner, Cowie, & Wainscoat 1993; Soifer et al. 1994; Djorgovski et al. 1995), and spectroscopic surveys to $K < 20$ (Songaila et al. 1994), $I < 22$ (Crampton et al. 1995) and to $B < 24$ (Glazebrook et al. 1995a). These data provide useful constraints for both cosmological models and galaxy evolutionary models.

As soon as deep optical counts of galaxies became available, it was realized that no-evolution (nE) models, i.e. models in which the absolute brightness and the spectra of galaxies do not change in time, predict a surface density of galaxies at faint magnitude significantly lower than the observations (see the review by Koo & Kron 1992). The excess in the observed number counts with respect to the nE model predictions is of the order of ~ 4 to 5 at $b_j \sim 24$ and ~ 5 to 10 at $b_j \sim 26$ (Maddox et al. 1990; Guiderdoni & Rocca-Volmerange 1991, hereafter GRV91).

Simple pure luminosity evolution (PLE) models, which

allow for brightness and spectral evolution in the galaxy population, were shown to provide a better fit to the faint galaxy number counts (Tinsley 1980; Bruzual & Kron 1980 (hereafter BK80); Koo 1981, 1985). However, these early PLE models were ruled out on the basis of comparisons with the results of z surveys of faint galaxies (Broadhurst, Ellis, & Shanks 1988; Colless et al. 1990; Koo & Kron 1992 and references therein), which failed to reveal the large number of high z galaxies predicted by the models. The z distributions in these surveys appeared to be in agreement with the predictions of nE models.

In an attempt to explain all aspects of the data with a single model, this apparent paradox (counts require PLE model but z distribution only admits nE model) prompted the development of a number of less straightforward models. These models relax some of the assumptions adopted in nE and PLE models, such as, the constancy of the volume number density of galaxies, and/or the standard cosmology. The excess observed in the faint counts can be explained, for example, by either non-conservation of the number of galaxies due to merger events (GRV91; Broadhurst, Ellis, & Glazebrook 1992; Carlberg & Charlot 1992) or dwarf galaxies which have faded and/or disappeared in recent epochs (Broadhurst et al. 1988; Cowie, Songaila & Hu 1991; Babul & Rees 1992). Fukugita et al. (1990) have proposed to revise the cosmological model introducing a non-zero cosmological

constant.

More recent and refined versions of PLE models have shown that at least some of the discrepancies with existing data can be substantially reduced also in the framework of these models (Guiderdoni & Rocca-Volmerange 1990 (hereafter GRV90); Gronwall & Koo 1995 (hereafter GK95); Metcalfe et al. 1991, 1995a).

The main goal of this paper is to explore up to what extent the properties of the faint galaxy samples can be understood in the framework of PLE models, without invoking the more exotic scenarios proposed in the literature. We examine a new set of PLE models and compare their predictions with the most recent data, including counts in all available photometric bands, and colours and z distributions as a function of magnitude for various samples, selected in different bands. A global comparison of this kind is essential because each different data set provides constraints on different PLE model parameters.

We find that standard PLE models built along the lines described by BK80, but with mild galaxy evolution, similar to that *assumed* by Metcalfe et al. (1991, 1995a), but *derived* here consistently from the Bruzual & Charlot (1993, hereafter BC93) spectral evolution models, provide satisfactory fits to most of the observational data in an $\Omega \sim 0$ universe. The only data set which our models do not reproduce well is the z distribution of the K -selected sample for $K > 17$ by Songaila et al. (1994). Despite this failure, and before new samples either confirm or modify the Songaila et al. results, we think that it is useful to compare the faint galaxy surveys with the predictions of simple PLE models in order to constrain the range of evolutionary and cosmological parameters used in these models.

In §2 we describe the main ingredients of our PLE model, i.e. the shape and normalization of the luminosity function of galaxies of various morphological types and the adopted models for their spectral evolution. In §3 we compare the predictions of our models with the observational data. The conclusions of our work are presented in §4.

2 STANDARD PLE MODELS

Standard PLE models (BK80; Metcalfe et al. 1991) assume that galaxies maintain at every z the same proportion of the various morphological types as observed locally ($z = 0$), and that the spectral evolution of these galaxies is well described by models which at low z reproduce the colours and k -corrections determined from observed galaxy spectra. Assuming a geometry for the universe, and scaling the galaxy luminosity function (LF) to match the number counts at a given magnitude in a specific band, one can compute the expected galaxy number counts in various bands, as well as the colour and z distributions as a function of magnitude.

2.1 Modelling faint galaxy counts and colour and z distributions

In a homogeneous and isotropic universe, the number of galaxies of each type brighter than a given magnitude m can be calculated from the integral

$$N_i(< m) = \int_o^{z_{max}} \int_{M_{min}}^{M_{max}(m, z)} \phi_i(M) dM \frac{dV(z, \Omega)}{dz} dz, \quad (1)$$

where $\phi_i(M)$ and $dV(z, \Omega)$ are, respectively, the local LF for the type and the comoving volume element. In this paper we will consider only the standard ($\Lambda = 0$) Friedmann cosmology defined by H_0 and Ω . We use $H_0 = 50 \text{ km s}^{-1} \text{ Mpc}^{-1}$ throughout this paper.

The total number of galaxies brighter than m , $N(< m)$, is obtained by adding $N_i(< m)$ over all types considered. From (1) we obtain the z -distribution $N_i(< m; z, z + dz)$ by integrating over the specific z range $(z, z + dz)$. In (1) $z_{max} = \min(z_f, z_L)$, where z_f is the assumed z of galaxy formation and z_L is the value of z at which the Lyman continuum break is shifted to the effective wavelength of the filter being considered, and the galaxy presumably becomes dark (Madau 1995). We use the following filters: U (Koo 1981), B and V (Buser 1978), b_j and r_f (Couch & Newell 1980), I and K (Wainscoat & Cowie 1992). For the U , b_j , r_f , I , and K bands, $z_L \simeq 3, 4, 6, 8$, and 23, respectively.

The integration over dM in (1) extends up to

$$M_{max}(m, z) = m - 5 \log \frac{d_L(z; H_0, \Omega)}{10} - corr(z; H_0, \Omega, z_f), \quad (2)$$

where $d_L(z; H_0, \Omega)$ is the luminosity distance measured in pc, and $corr(z; H_0, \Omega, z_f)$ is the *correction* needed to obtain the galaxy rest frame magnitude from its observer frame magnitude. In the nE model, it is just the k -correction. In the PLE model, it is given by the $(e + k)$ -correction, which also includes the effects due to the intrinsic galaxy luminosity evolution. We computed this correction up to $z = z_{max}$ from the synthetic spectral energy distribution (SED) of the various galaxy types for each photometric band.

Finally, the colour distribution $N_i(< m; c, c + dc)$ can be derived from the z distribution $N_i(< m; z, z + dz)$ for each type of galaxy by using the cosmology dependent relation between colour and z , $c_i(z; H_0, \Omega, z_f)$, given by the adopted spectral evolution model. The colour distributions for the different types are then added up.

2.2 Luminosity function

There is increasing evidence that the galaxy LF varies with galaxy type. Bingelli, Sandage & Tamman (1988) have derived morphology dependent LFs for galaxies in the Virgo cluster. Efstathiou, Ellis & Peterson (1988), Shanks (1990) and Loveday et al. (1992) have shown that the LF in the field is well described by the analytical expression of Schechter (1976), with values of α and M^* which depend on the galaxy morphological type. In general, blue galaxies show a steeper slope than red galaxies.

We adopt the values of α and $M_{b_j}^*$ derived separately for early and late type galaxies by Efstathiou et al. (1988) from the Anglo-Australian Redshift Survey data, listed in Table 1. We assume that these parameters are valid from $M_{b_j} = -24$ to $M_{b_j} = -15.5$ (cf. Loveday et al. 1992). To obtain the local LF in the U , r_f , I , and K bands we shift $M_{b_j}^*$ according to the colours at $z = 0$ for each galaxy type listed in Table 1. The K band LF thus obtained is consistent with the observed one (Mobasher et al. 1995; Glazebrook et al. 1995b).

We have not used the more recent determination of α and $M_{b_j}^*$ by Loveday et al. (1992), because of the bias mentioned by these authors against identifying early-type galaxies in their sample. As shown by Zucca, Pozzetti & Zamorani

Table 1. Local galaxy mix, LF parameters^a, and local colors^b

Type	Fraction ^c	α	$M_{b_j}^*$	Φ_i^*	$B - V$	$U - b_j$	$b_j - r_f$	$b_j - I$	$b_j - K$
E/S0	0.28	-0.48	-20.87	0.95	0.95	0.75	1.55	2.32	4.13
Sab-Sbc	0.47	-1.24	-21.14	1.15	0.68	0.32	1.21	1.83	3.47
Scd-Sdm	0.22	-1.24	-21.14	0.54	0.43	-0.05	0.88	1.39	2.96
very Blue (vB)	0.03	-1.24	-21.14	0.12	0.07	-0.49	0.32	0.63	2.06

^a α , $M_{b_j}^*$ from Efstathiou et al. (1988); Φ_i^* in units of 10^{-3} Mpc $^{-3}$ (§2.3). $H_0 = 50$ km s $^{-1}$ Mpc $^{-1}$ throughout this paper;

^b From BC93 ($t_g = 16$ Gyr, $z_f = 4.5$, $\Omega = 0$);

^c Mix from Ellis (1983).

(1994), the correction for this bias moves the Loveday et al. values of (α , M^*) towards those of Efstathiou et al. (1988).

2.3 Count normalization

The uncertainties in the normalization of the local galaxy LF translate into a major source of uncertainty in the models for faint galaxy counts. Moreover, different selection effects in photographic and CCD data may lead to difficulties in comparing bright and deep surveys (McGaugh 1994). The reduced size of well calibrated samples at bright magnitude and the local fluctuations caused by galaxy clustering lead to large variations in the bright counts. In principle, this problem would be avoided by using the APM galaxy counts in the range $15 < b_j < 20.5$ derived from 4300 deg 2 of the sky (Maddox et al. 1990). However, while these counts are close to the mean of previously published data at $b_j \sim 19 - 20$, they show a steeper slope for $b_j < 19$ than previous determinations. Thus, the APM counts at $b_j < 17$ are below models normalized to match the counts at $b_j = 19 - 20$. Metcalfe, Fong & Shanks (1995b) show evidence of a possible magnitude scale error in the APM galaxy survey, whose size could be large enough to cause the apparent disagreement between the APM galaxy counts and the predictions from standard models in the range $17.5 < b_j < 20$.

Because of this uncertainty in the counts at bright magnitude, we have chosen to scale our model predictions to the observed number counts in the range $19 < b_j < 19.5$, namely $\log N_0 = 1.98$ gal deg $^{-2}$ (0.5 mag) $^{-1}$ (see also GRV90). This normalization is consistent with that obtained recently for the K band LF (Glazebrook et al. 1995b), as well as for the b_j band (Ellis et al. 1995).

Finally, in order to compute Φ_i^* , i.e. the normalization of the LF for each morphological type, we have adopted the local galaxy mix derived by Ellis (1983) for $b_j < 16.5$ from the DARS data (see column 2 in Table 1). This galaxy mix is in good agreement with the percentage of elliptical and spiral galaxies derived recently by Efstathiou et al. (1988). The same values of Φ_i^* are used to model different photometric bands. The b_j LF summed over all types derived from our models is well described by the parameters $\alpha = -1.2$, $M_{b_j}^* = -21.1$, $\Phi_{ALL}^* = 2.5 \times 10^{-3}$ Mpc $^{-3}$.

2.4 Spectral energy distributions

Our galaxy spectral energy distributions (SEDs) are based on the BC93 galaxy spectral evolution library. The BC93

models are built from a library of stellar tracks which includes all evolutionary stages for stars of solar metallicity. Empirical near-UV to near-IR spectra of galactic stars, extended to the far-UV by means of model atmospheres, are used in the synthesis. The inclusion in these models of the Post-AGB stellar evolutionary phase, which contributes significantly in the UV spectral range in old stellar populations (Magris & Bruzual 1993), represents an improvement over previous spectral evolution codes.

We used the following procedure to select a subset of galaxy models from the BC93 library. First, we selected models on the basis of their ability to reproduce the shape of the continuum and spectral features in the SEDs of local galaxies of different morphological types, and verified that the k -corrections computed from the models were in agreement with the empirical ones. Then, among these models we selected by trial and error those which reproduced better the empirical constraints on galaxy evolutionary properties, namely, galaxy number counts and colour and z distributions.

Thus, we have to compute the number count model as outlined in §2.1 in order to find which galaxy spectral evolution models produce the best fit to the counts and colour and z distributions. The feedback in this procedure is unavoidable due to the lack of independent constraints on galaxy evolution (BK80, GK95).

2.4.1 Evolutionary constraints on the SEDs

The following aspects of the data guided our choice of the SEDs. Strong evolution for $z < 1$ is ruled out for all galaxy types by the observed z distributions of Broadhurst et al. (1988) and Colless et al. (1990, 1993), which are close to the nE prediction up to $b_j = 22.5$. Colless et al. (1993) estimate an upper limit to the amount of luminosity evolution of $\Delta M_B \sim -1.2$ for $z < 1$, providing a strong constraint to the evolutionary corrections. The observed number counts, particularly in the b_j band, require optically mildly-evolving SEDs, over the entire z range, in agreement with Koo, Gronwall, & Bruzual (1993, hereafter KGB93). Additional evidence in favor of mild evolution derives from recent work on the z evolution of the LF in B -, I -, and K -selected samples by Colless (1995), Lilly et al. (1995b), and Glazebrook et al. (1995b), respectively.

We introduce the spectral class of very Blue (vB) galaxies in order to explain the bluest colours, $b_j - r_f \lesssim 0.3$, ob-

Table 2. Initial mass function^a

IMF	x_i	m_1	m_2	c_i
Scalo (1986)	-2.60	0.10	0.18	100.530
	0.01	0.18	0.42	1.14430
	1.75	0.42	0.62	0.25293
	1.08	0.62	1.18	0.34842
	2.50	1.18	3.50	0.44073
	1.63	3.50	125	0.14819
	Salpeter (1955)	1.35	0.10	125
				0.17038

^a $f_i(m) = c_i m^{-(1+x_i)}$ for $m_1 \leq m \leq m_2$, m_1 and m_2 in M_\odot units.

served in the deepest b_j -selected surveys (Glazebrook et al. 1995a). vB galaxies are meant to reproduce a population of starburst galaxies present at each z , whose evolution does not follow the pure luminosity prescription. We assume that star formation in these galaxies keeps their SED constant in time. For vB galaxies we adopt the LF of spiral galaxies. The observed fraction of galaxies bluer than $B - V = 0.6$ at the faint magnitude limit ($\sim 10\%$), is reproduced assuming that vB galaxies represent $\sim 3\%$ of the total local mix (Table 1). Thus, at the few % level, our PLE models include a fraction of non-passively evolving galaxies.

3 RESULTS

3.1 Reference models

A BC93 galaxy evolution model is specified by the star formation rate (SFR) $\psi(t)$ and the initial mass function (IMF). Once H_0 , Ω , and z_f are specified, the age t_g of the model SEDs and their observer frame properties are fixed. We considered models with $t_g = 16$ and 12.7 Gyr, corresponding to $z_f = 4.5$ and 10 for $\Omega = 0$ and 1, respectively. We tested models computed for the Salpeter (1955) and the Scalo (1986) IMFs (Table 2). Table 3 defines the BC93 model SEDs selected as described in §2.4 that will be used to build our reference models for the counts as indicated in §2.1. A brief comment on these SEDs follows.

Models for E/S0 and Sab-Sbc galaxies are characterized by the SFR $\psi(t) \propto \tau^{-1} \exp(-t/\tau)$, where τ is the e-folding time characterizing this form of $\psi(t)$. The spectral properties of nearby E/S0 galaxies are reproduced well by both the $\tau = 1$ Gyr model (hereafter τ_1 model) and a model in which star formation takes place at a constant rate during the first Gyr in the life of the galaxy (hereafter B_1 model) for either the Salpeter or the Scalo IMF, and by the $\tau = 2$ Gyr model (or τ_2 model) for the Scalo IMF. The observed $b_j - r_f$ and $B - K$ colour distributions are reproduced more closely by our $\Omega = 0$ reference PLE model if we represent the E/S0 galaxy SEDs by the τ_1 and τ_2 models, rather than by the B_1 model (Table 3).

The local properties of Sab-Sbc galaxies are well described by the $\tau = 4$ Gyr (or τ_4) Salpeter IMF model, or the $\tau = 10$ Gyr (or τ_{10}) Scalo IMF model. The Scd-Sdm galaxies are described satisfactorily by a model in which stars form at a constant rate following the Salpeter IMF (hereafter *cons* model). The SED of the vB galaxies can be approximated by a model with constant SFR seen at an age

Table 3. Galaxy SED model parameters

Ω	Type	SFR	IMF	t_g (Gyr)
0	E/S0	τ_1, τ_2	Scalo	16
	Sab-Sbc	τ_{10}	Scalo	16
	Scd-Sdm	cons	Salpeter	16
	vB	cons	Salpeter	0.1
1	E/S0	B_1, τ_1	Scalo	12.7
	Sab-Sbc	τ_8	Scalo	12.7
	Scd-Sdm	cons	Salpeter	12.7
	vB	cons	Salpeter	0.1

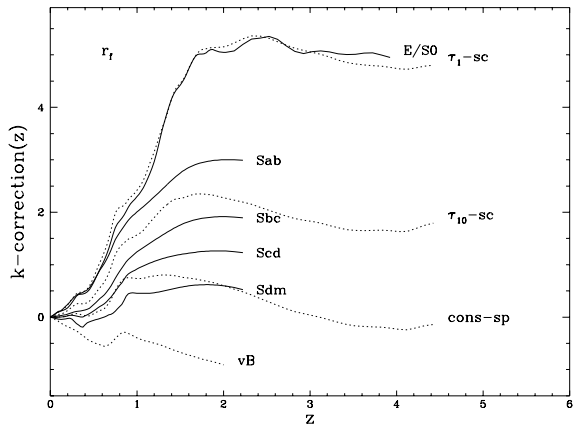


Figure 1. k -correction in the r_f band for galaxies of different morphological types from BC93 models (dotted lines, *sc*: Scalo IMF; *sp*: Salpeter IMF) and from the observed SEDs described in the text (solid lines).

of 0.1 Gyr after the last major event of star formation. This SED is even bluer than that of NGC 4449 (BC93).

3.1.1 Scalo IMF vs. Salpeter IMF

The constraints mentioned in §2.4 led us to adopt Scalo IMF models for early-type galaxies (Table 3). The Scalo IMF is less rich in massive stars than the Salpeter IMF because of the steeper slope of the former at the high mass end. The high number of massive stars in the Salpeter IMF models produces a large amount of UV flux at early times, making high z E galaxies detectable in current deep surveys and producing an excess in the faint b_j counts with respect to the observations. An alternative way to reduce the UV flux is to assume a significant amount of dust extinction inside the galaxies (GK95).

There is some ambiguity in the literature on the functional form of the Scalo IMF. Following a suggestion by D.C. Koo, BC93 have divided the IMF given by Scalo in graphical form into the 6 different segments listed in Table 2. For the i^{th} -segment the IMF is given by $f_i(m) = c_i m^{-(1+x_i)}$. The constants c_i are computed from the requirement of continuity of the IMF (cf. Guiderdoni & Rocca-Volmerange 1987, hereafter GRV87).

Table 4. Intrinsic luminosity evolution

λ_0^a	2300Å	1150Å	11000Å	5500Å
Type	$\Delta B_{z=1}$	$\Delta B_{z=3}$	$\Delta K_{z=1}$	$\Delta K_{z=3}$
E/S0	-1.6	-6.0	-0.6	-2.3
Sab-Sbc	-1.0	-1.6	~ 0	~ 0
Scd-Sdm	~ 0	~ 0	+0.4	+0.6

^a Rest frame wavelength

3.2 k and $(e+k)$ -corrections

Fig 1 shows the model and the empirical k -corrections in the r_f band. These models, listed under $\Omega = 0$ in Table 3, reproduce the flattening at high z shown by the empirical k -corrections of ellipticals and spirals (cf. Cowie et al. 1994). In contrast, the k -corrections of ellipticals modeled by Rocca-Volmerange & Guiderdoni (1988) continue to increase with z . This difference is mainly due to the lower UV flux in the GRV87 model for E galaxies, resulting from the lack of Post-AGB stars in their population synthesis.

The k -corrections derived from the synthetic spectra are in agreement with the k -corrections in the (U, b_j, r_f, I) bands computed from the observed spectra of Pence (1976) up to $z = (0.6, 0.9, 2.2, 2.5)$, with the compilation in b_j by King & Ellis (1984) up to $z = 1.5$, and with the K and B band estimates by Cowie et al. (1994) up to $z < 3$. Our E/S0 models reproduce also the k -correction at higher z computed from the average observed E galaxy SED of BC93.

Figures 2a and 2b show the k and $(e+k)$ corrections in the b_j and K bands, respectively, for the SEDs selected in the $\Omega = 0$ case (Table 3). We see here the flattening of the $(e+k)$ -corrections in b_j and r_f at high z , which was assumed entirely *ad hoc* by Metcalfe et al. (1991, 1995a). If we use Salpeter IMF models for the Ellipticals, the $(e+k)$ -correction in b_j continues to decrease with z , up to $\sim -3(-4)$ at $z = 2(3)$.

The difference between the $(e+k)$ and k -corrections gives the intrinsic galaxy luminosity evolution, or $\Delta M_z = e\text{-correction}(z)$. This quantity represents the luminosity brightening of a galaxy at $\lambda_0 = \lambda_{\text{obs}} \times (1+z)^{-1}$ with respect to its $z=0$ luminosity at the same wavelength. The e -corrections at $z=1$ and 3 , as observed in the B and K bands are given in Table 4. The amount of brightening up to $z=1$ is relatively small, as required by the observed z distributions. For $z \sim 3$, $\Delta B_z \sim -6$ for E/S0 galaxies and $\Delta B_z \sim -1.6$ for Sab-Sbc galaxies. In the K band the luminosity evolution is significantly lower than in the other bands ($\Delta K_{z=1} \sim -0.6$ and $\Delta K_{z=3} \sim -2.3$ for E/S0 galaxies), showing how the concept of mild luminosity evolution depends on the wavelength range being considered.

3.3 Number counts

Optical counts have reached very deep levels thanks to CCD cameras. IR array detectors have made possible to extend the faint galaxy work to the K band. Observations in the K band are particularly important because light at $2\mu\text{m}$ is relatively insensitive to dust extinction. At high z the K band samples the well understood rest frame optical range,

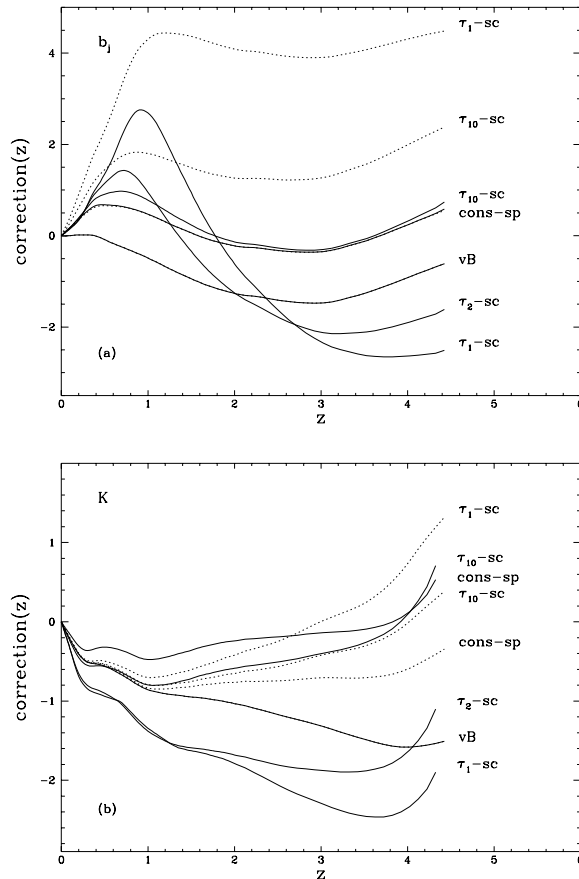


Figure 2. (a) b_j band $(e+k)$ -corrections (solid lines) and k -corrections (dotted lines) for galaxies of different morphological types derived from the BC93 models listed under $\Omega = 0$ in Table 3. (b) Same as (a) but for the K band.

Table 5. Slope γ at faint magnitudes

Band	mag. range	γ_{obs}	γ_{PLE}^a	γ_f^b
U	20–25	0.49	0.49	0.22
b_j	20–25	0.45	0.46	0.30
r_f	20–25	0.37	0.36	0.21
I	19–23	0.34	0.35	0.17
K	18–23	0.26–0.30	0.29	0.10

^a From the $\Omega = 0$ reference PLE model

^b Predicted slope at faint limits: $24 < m < 27$

in which spectral evolution is less significant than in the UV region sampled at high z by the optical bands (Table 4). K band counts are thus less sensitive than optical counts to the evolution of the stellar population and to the details of the SFR and IMF. K counts can therefore be used, at least in principle, as a direct test of cosmological models. Because of these reasons in this paper we pay special attention to fitting at the same time all known properties of faint galaxy samples, from the U to the K band.

Figures 3a-e show the differential number counts in the (U, b_j, r_f, I, K) bands. As in most observational papers, from which the data have been taken, $N(m)$ is plotted per

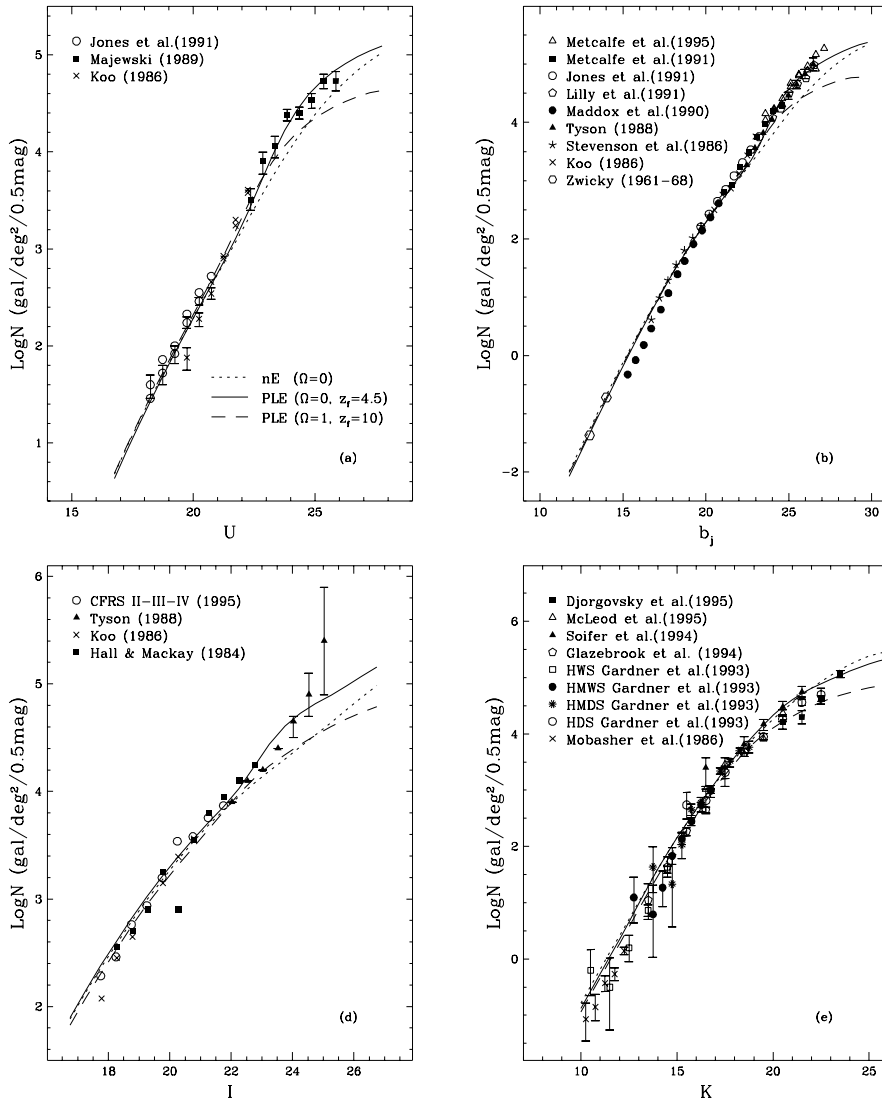


Figure 3. Differential galaxy number counts per square degree per half magnitude interval as a function of apparent magnitude. The sources of the observed data points are indicated in each panel. The lines show the predicted counts for different models: dotted line: nE model ($\Omega = 0$, $z_f = 4.5$); solid line: PLE model ($\Omega = 0$, $z_f = 4.5$); dashed line: PLE model ($\Omega = 1$, $z_f = 10$). (a) U band. (b) b_j band. (c) r_f band. (d) I band. (e) K band.

half magnitude bin. The sources of the data points are indicated in the figures. Even though in a few cases the counts from different groups show a relatively large scatter, the slope γ of the $\log N - m$ relation is reasonably well defined in all bands. At bright magnitude $\gamma \sim 0.6$ is close to the Euclidean value. Table 5 shows that at fainter magnitude γ decreases with increasing filter effective wavelength (Jones et al. 1991; Gardner et al. 1993; Djorgovski et al. 1995). Despite the large difference in γ between b_j and K , the two bands are sampling the same galaxy population. We verified that the observed b_j counts can be reproduced (in number and γ) by just shifting the observed K band counts according to the $(B - K)_{med}$ at a given K given by Gardner et al. (1993). The lines in these figures represent the predictions

of the models that are described in detail below.

3.3.1 *nE* model

The well known excess of faint galaxies above the nE model prediction is confirmed (Fig 3). In nE models the SEDs of distant galaxies are represented by SEDs that match those of nearby galaxies (Table 3), which correspond, on average, to old stellar populations. The amount of UV flux produced by Post-AGB stars in E/S0 galaxies is not as large as that attained at early ages. The large k -correction moves these galaxies towards fainter magnitude and, hence, they do not contribute to the predicted counts even at the faint limit reached by current observations.

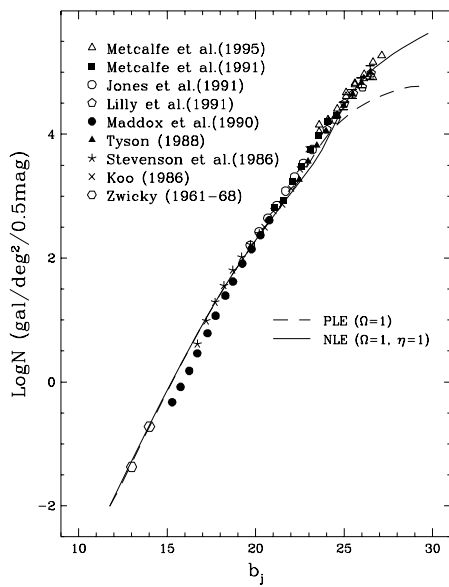


Figure 4. Differential galaxy number counts as a function of b_j apparent magnitude. The lines show the predicted counts for two different models: solid line: NLE model ($\Omega = 1$, $z_f = 10$, $\eta = 1$); dashed line: PLE model ($\Omega = 1$, $z_f = 10$).

The excess of galaxies with respect to our nE model (with $\Omega = 0$) is about a factor of 2 at $m \sim 24$ in all bands, except for the K band in which the nE model is consistent with the data. Even at fainter magnitude the observed data are never more than a factor of three higher than the nE model. The excess reported by other authors (Broadhurst et al. 1988; Maddox et al. 1990; GRV90) is larger by a factor ~ 2 than our result. This difference is mainly due to our choice of normalizing the model counts to the observed number in the range $19.0 < b_j < 19.5$ (§2.3), and to

our selection of realistic SEDs for early-type galaxies. Our SEDs reproduce reasonably well the UV flux of local galaxies, which translates into significant differences between our k -corrections at high z and those used in the quoted papers. On the other hand, our results are in reasonable agreement with the nE model of KGB93, supporting their conclusion that only a moderate amount of spectral evolution is required by the data.

In an $\Omega = 1$ universe the difference between data and model (not shown) at faint magnitude is substantially higher, being a factor of $\sim 3(4)$ at $b_j \sim 24(26)$.

3.3.2 PLE models

From Figures 3a-e we see that the $\Omega = 0$ reference PLE model reproduces reasonably well the observed galaxy counts in the five bands over a wide magnitude range. The most significant discrepancies are with respect to the bright b_j counts of Maddox et al. (1990, §2.3), and in K with respect to the Mobasher et al. (1986) counts and the Gardner et al. (1993) HWS counts. At $K > 20$ the model agrees well with the data from Soifer et al. (1994) and McLeod et al. (1995), but overestimates the Gardner et al. (1993) HDS data and the Djorgovski et al. (1995) counts for $K < 23$. Table 5 shows the excellent agreement between the observed and predicted values of the slope γ in the five bands. At fainter magnitude than the current limits the model predicts a significant flattening of $N(m)$ in all bands (last column of Table 5). The faintest r_f and I band counts of Tyson (1988) do not show this flattening but show an excess (with large error bars) with respect to the model predictions. If faint counts keep increasing with a steep slope, then higher values of z_f are likely needed to fit the data. For increasing z_f , the flattening predicted at faint magnitude shifts towards even fainter magnitude. Deeper data are necessary to test these predictions in detail.

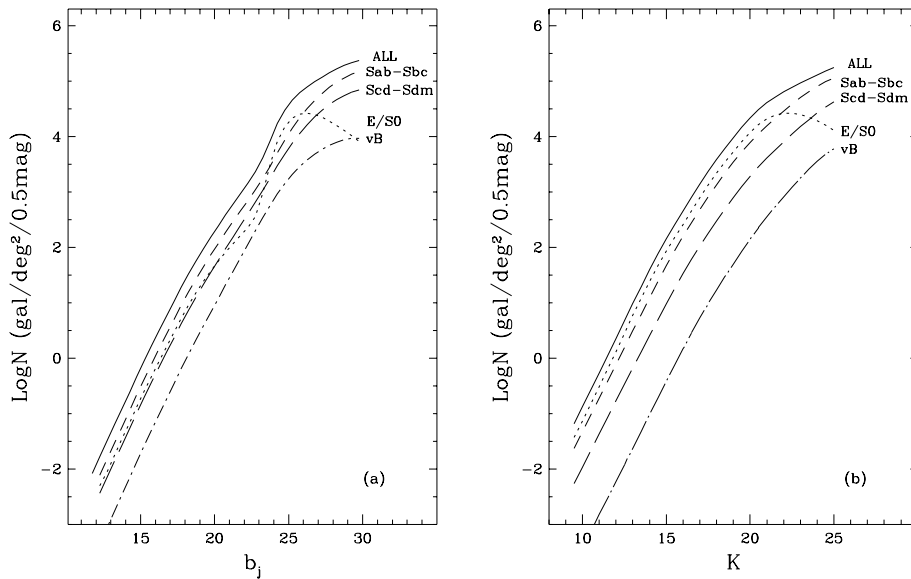


Figure 5. Contribution of each morphological type to the total differential galaxy number counts as a function of apparent magnitude. The lines show the predicted counts for the reference $\Omega = 0$ PLE model. Total counts: solid line; E/SO: dotted line; Sab-Sbc: short-dashed line; Scd-Sdm: long-dashed line; vB: dot-dashed line. (a) b_j band. (b) K band.

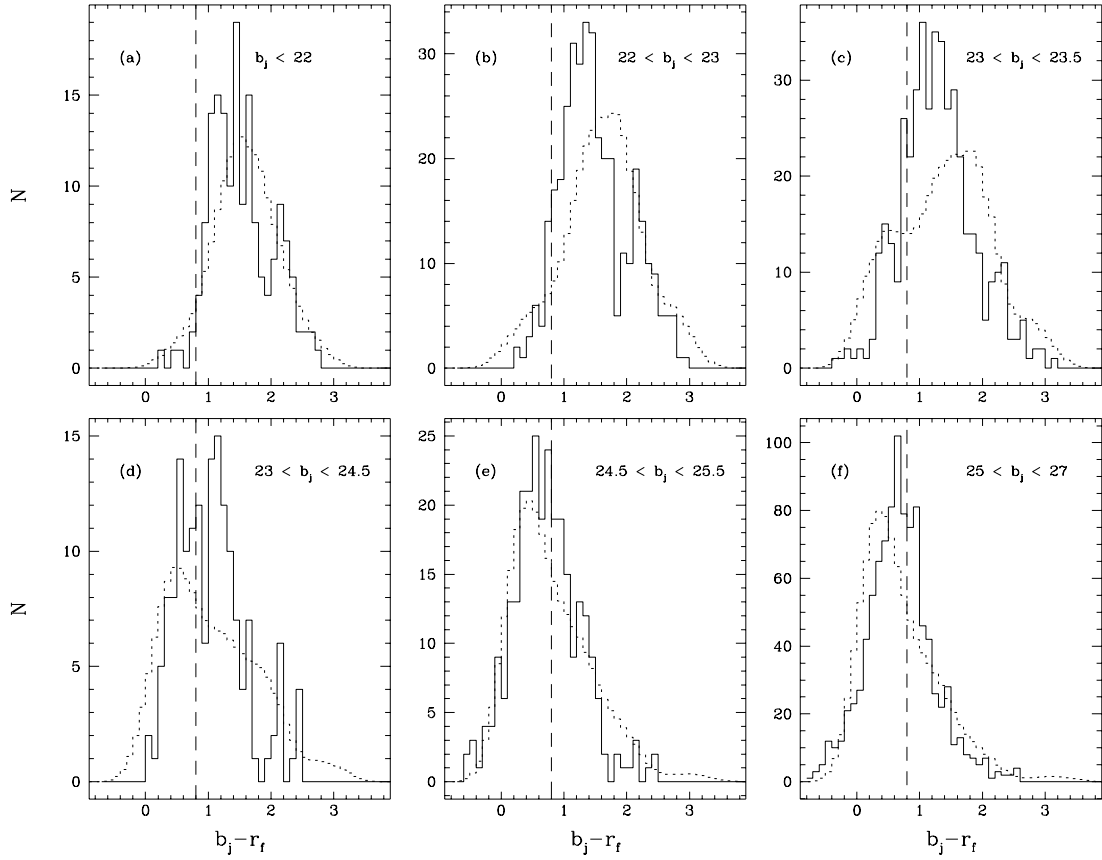


Figure 6. $b_j - r_f$ colour distribution for different b_j bins. The solid histograms show the observed distributions from Metcalfe et al. (1991, 1995a) and, for the faintest bin, from Koo & Kron (1992; data kindly provided to us by C. Gronwall). When needed, the data have been converted to the b_j and r_f passbands of Couch & Newell (1980). The dotted histograms show the predictions of the $\Omega = 0$ reference PLE model. To aid the eye a dashed line is drawn at $b_j - r_f = 0.8$.

In Figures 3a-e we see that the $\Omega = 1$ model significantly underestimates the faint counts in all bands. Although to a lesser extent, this is even true in the K band, where the influence of evolution is less important. The deficiency in the counts for the $\Omega = 1$ model is due to the decreasing comoving volume available for increasing Ω . The differences between the predictions of this model and the data are minimized assuming a high z_f . Even for $z_f = 10$ the excess in the observed counts is ~ 3 at $b_j = 26$.

3.3.3 Number luminosity evolution (NLE) model

Models that obey the $\Omega = 1$ constraint of the inflation scenario require physical effects not considered in simple PLE models. Among several possibilities, strong galaxy merger events at early ages have been suggested (Rocca-Volmerange & Guiderdoni 1990 (hereafter RVG90); Broadhurst et al. 1992). To test qualitatively this possibility, we have constructed a NLE model in which the LF is allowed to evolve with z as proposed by RVG90

$$\phi(L, z) = (1+z)^{2\eta} \phi[L(1+z)^\eta, z=0]. \quad (3)$$

This function simulates the merging of faint high z galaxies to form bright local galaxies, while conserving the total

comoving mass density. We have used the same galaxy evolution models as in the PLE models (Table 3). This simple and crude NLE model fits the galaxy counts quite well in all bands. A good fit is obtained for $\eta = 1$ in (3). Fig 4 shows the resulting b_j counts. More realistic models that simulate the change of the photometric properties of the merging galaxies have to be computed (cf. Fritze-v.Alvensleben & Gerhard 1994).

3.3.4 Contribution of each galaxy type to the total counts

Fig 5 shows the contribution to the total b_j and K counts of each galaxy type in the $\Omega = 0$ PLE model. In b_j and U (not shown), early spirals are the dominant population over most of the magnitude range. Evolved E/S0s contribute only $\sim 20\%$ to the counts at $20 \leq b_j \leq 22$. Young E/S0 galaxies at their maximum SFR period contribute $\sim 50\%$ and produce the hump in the total counts in the range $23.5 \leq b_j \leq 25.5$. This hump has been noticed by Metcalfe et al. (1995a) in their counts. E/S0 galaxies are also dominant for $K \lesssim 22$. There is no K hump because even at $z = z_f = 4.5$ the K filter samples the blue spectral region, not reaching the UV rest frame and missing the signature of the high star formation episode. The hump shifts

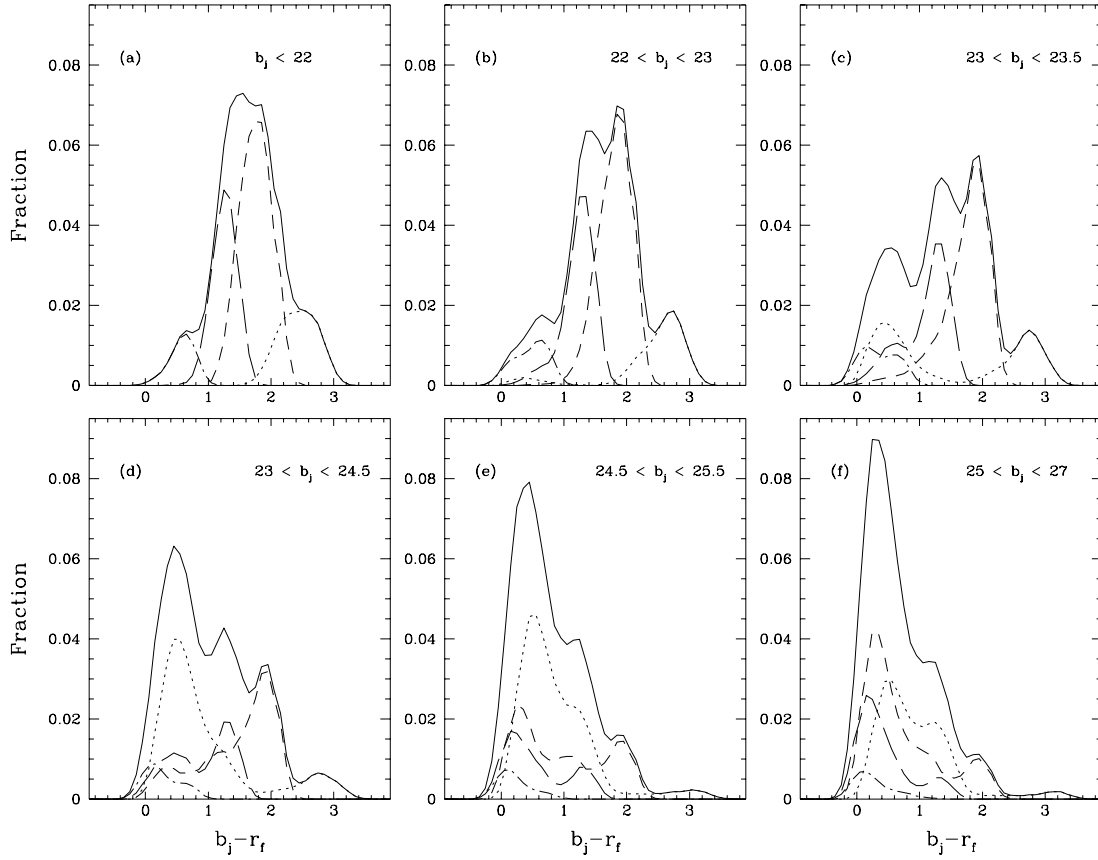


Figure 7. $b_j - r_f$ predicted colour distribution for the various morphological types in different b_j bins for the $\Omega = 0$ reference PLE model. All galaxies: solid line; E/S0: dotted line; Sab-Sbc: short-dashed line; Scd-Sdm: long-dashed line; vB: dot-dashed line.

to brighter magnitude for higher Ω and to fainter magnitude for higher z_f . The onset of the b_j hump may seem particularly steep in our models because we use a coarse grid of galaxy types. With a finer grid of galaxy spectra the bright galaxy phases appear more gradually and the onset of the hump is less evident (GK95). The hump in the data (Fig 3b) suggests some degree of discreteness in the distribution of galaxy types, intermediate between ours and GK95's.

3.4 Colour distributions

The colour distributions derived from faint galaxy surveys show a gradual trend towards bluer mean colours at fainter magnitude. The result that $b_j - r_f$ (photographic) becomes significantly bluer beyond $b_j \sim 22$ (Kron 1980), has been confirmed by various groups (Shanks et al. 1984; Tyson 1984; Infante, Pritchett & Quintana 1986). With CCD detectors colour distributions have been extended up to $b_j \sim 27$ (Koo & Kron 1992 and references therein; Metcalfe et al. 1995a). The median $B - K$ colour of K -selected field galaxies also becomes bluer beyond $K \sim 17.5$ (Gardner et al. 1993). To make the comparison of the data and models more realistic, we have applied a gaussian error function with $\sigma = 0.15$ mag to the colour vs. z relations before deriving the colour distributions. This procedure is expected to take into account, at least to first order, both the obser-

vational errors in the colours and the intrinsic dispersion in the colours of galaxies of the same morphological type.

Fig 6 shows the $b_j - r_f$ colour distribution for different bins of b_j . At the brightest and faintest bins, panels (a), (d)-(f), the agreement between the data and model distribution is quite good. At intermediate magnitude, panels (b) and (c), the model distribution is redder than the data by $\sim \Delta(b_j - r_f) = 0.4$. Despite this discrepancy, the model predicts that galaxies with $b_j - r_f < 0.8$ appear at $b_j \sim 23$, and are essentially absent at brighter magnitude.

Fig 7 shows the $b_j - r_f$ fractional colour distribution predicted by the model for the same b_j bins of Fig 6 discriminated by galaxy morphological type. While at bright magnitude, panels (a) and (b), the various morphological types are reasonably well separated in colour, at the faintest bins, panels (e) and (f), galaxies of all types share the same colours. In particular, galaxies bluer than $b_j - r_f = 0.8$ are not just vB galaxies or late type spirals, but $\sim 50\%$ of them in panel (c) and about 60% in panel (d), are high z young E/S0 galaxies with $z_{med} \sim 1.5$. These are the same galaxies responsible for the blue (at high z) and the red (at low z) tails of the distribution in panels (c) and (d).

Fig 8 compares the Hawaii K -band survey (Songaila et al. 1994) $B - K$ colour distribution with our model. This

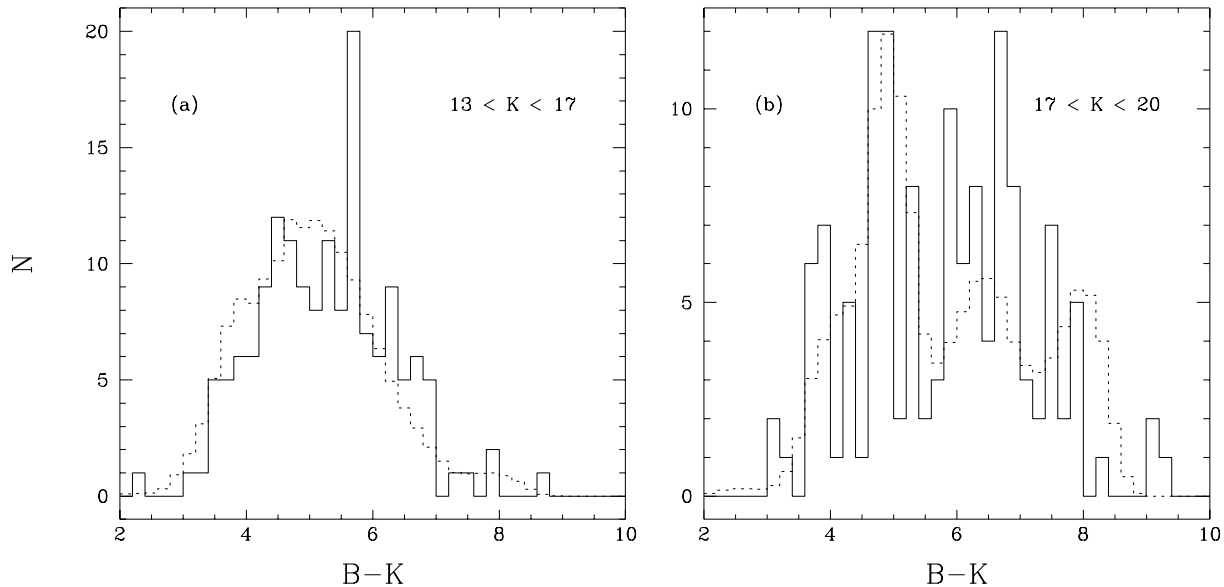


Figure 8. $B - K$ colour distribution for different K bins. The solid histograms show the observed distributions from the Hawaii K band survey (Songaila et al. 1994). The dotted histograms show the predictions of the reference $\Omega = 0$ PLE model.

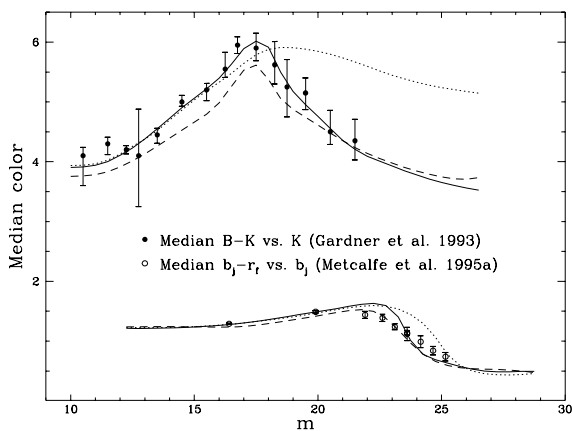


Figure 9. Median colours as a function of apparent magnitude. The bottom part of the figure shows $(b_j - r_f)_{med}$ vs. b_j . The top part shows $(B - K)_{med}$ vs. K . The data points are from the compilations by Metcalfe et al. (1995a) and Gardner et al. (1993). The lines show the predictions for the $\Omega = 0$ reference PLE model (solid line), $\Omega = 1$ reference PLE model (dashed line), $\Omega = 0$ nE model (dotted line).

sample has been obtained as a combination of a number of different K magnitude limited surveys. The size of the surveyed area was diminished as a function of limiting K to provide a roughly constant number of galaxies in each magnitude bin from $K = 13$ to $K = 20$. The model has been scaled to the number of galaxies observed in each bin. Also in this case the agreement between model and data is rather good.

Fig 9 shows the observed $(b_j - r_f)_{med}$ and $(B - K)_{med}$ median colours as a function of b_j and K . The $\Omega = 0$ PLE model reproduces rather well the data. High- z star forming

galaxies are responsible for blueing the median model colour at faint K . This is one possible reason why galaxies with colour as red as local E galaxies are not detected at faint K (Gardner 1995). The nE mode fails to reproduce the data, especially in $(B - K)_{med}$ vs. K , where the difference between the PLE and the nE models is large. Even though in the $\Omega = 1$ PLE model we have used intrinsically redder galaxy SEDs than in the $\Omega = 0$ model (Table 3), the median $B - K$ for the $\Omega = 1$ model is bluer than for the data. The main reason for this shift towards bluer colours in the $\Omega = 1$ model is the younger age of the galaxies in this cosmology, despite the higher z_f .

3.5 Redshift distributions

Multi-object spectrograph surveys of large samples of faint galaxies have reached faint enough magnitude for evolution to be detectable. At $b_j \gtrsim 21$ large numbers of $z > 1$ galaxies are predicted by PLE models in which galaxies undergo *strong* luminosity evolution (Broadhurst et al. 1988, 1992). The failure of the z surveys to reveal these galaxies sets strong upper limits on the amount of luminosity evolution that can be invoked to explain the excess in the number counts and the blueing of the median colour discussed in the previous sections. Rather than being evidence against all PLE models and in favour of the nE model, we argue below that the observed z distributions of blue-selected faint galaxies are consistent with PLE models in which galaxies evolve mildly in luminosity and rule out only the large amounts of luminosity evolution assumed in early PLE models.

3.5.1 b_j band

Fig 10 shows the z distributions derived from four surveys. Panels (a)-(c) correspond to b_j limited samples, while the

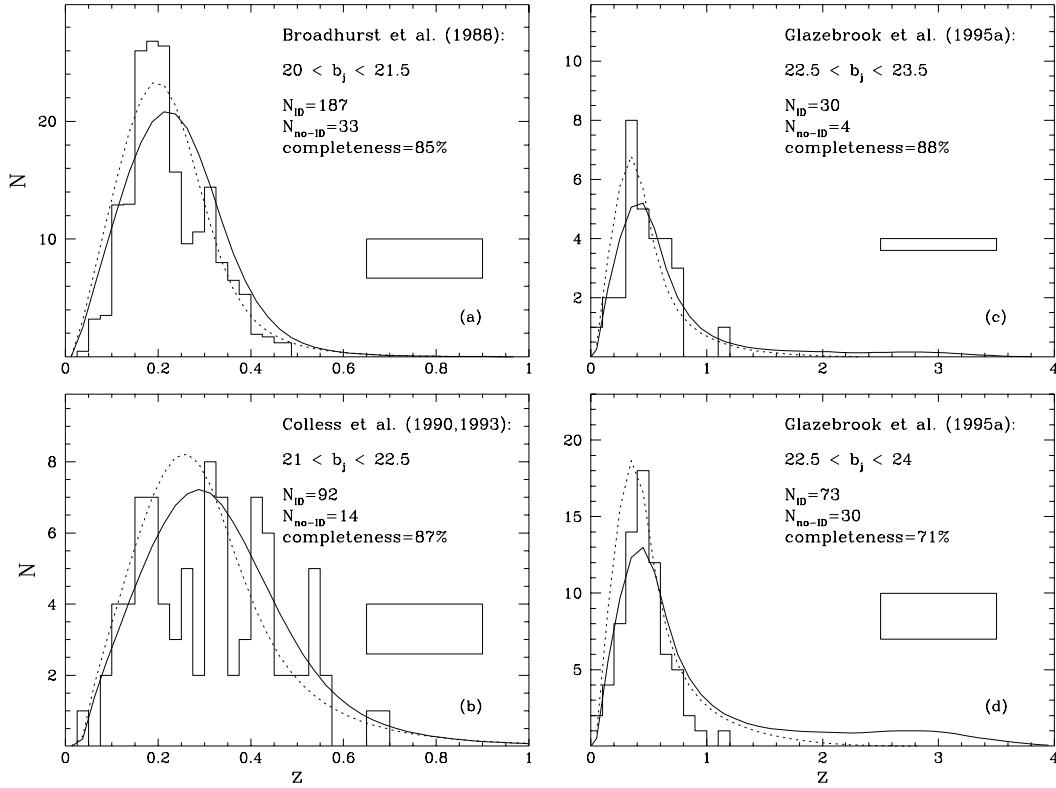


Figure 10. z distributions for b_j selected samples. The source for the observed distributions (solid histogram) is indicated in each panel together with N_{ID} = number of galaxies with measured z , N_{no-ID} = number of galaxies for which no z could be measured, and the completeness limit of the survey. The area of the rectangle in each panel = N_{no-ID} . Dotted line: nE model; solid line: PLE model; both for $\Omega = 0$, $z_f = 4.5$. The model predictions have been scaled to the total number of objects, $N_{ID} + N_{no-ID}$.

data in panel (d) are a combination of seven fields with different limiting magnitude, ranging from 23 to 24 in b_j , and completeness limit $> 70\%$ (Glazebrook et al. 1995a). In the latter case, our simulation includes the different b_j limiting magnitude for each field. The data in panel (b) correspond to the LDSS survey (Colless et al. 1990), supplemented with additional z measurements in a subsample of the original LDSS survey areas by Colless et al. (1993). The z distribution of the $\Omega = 0$ reference PLE model shown in panels (a) and (b) is consistent with the data, and does not show a significant high z tail. The mean z for the PLE model distribution in these two panels are $\langle z \rangle = (0.23, 0.32)$, in excellent agreement with the measured values (0.22, 0.31). Colless et al. (1993) reduced the z incompleteness in their LDSS subsample to 4.5%. From an analysis of these data they conclude that at most $\sim 4\%$ of galaxies with $b_j < 22.5$ have $z > 0.7$. The PLE model predicts $\sim 3\%$ of galaxies with $z > 0.7$ in this magnitude range.

At fainter magnitude, panels (c) and (d), the PLE model predicts a high z tail which is not seen in the data. Following Glazebrook et al. (1995a), we compare in Table 6 the values of z_{med} (median z) and $f_{0.7}$ (fraction of galaxies with $z > 0.7$) for their survey and our model. For each magnitude range in Table 6, the first line gives z_{med} and $f_{0.7}$ for the galaxies with measured z , the second line gives upper limits computed by assuming that all the z -unidentified galaxies are at $z > 0.7$, and the third line lists the predic-

Table 6. Glazebrook et al. (1995) z surveys

b_j range	source	z_{med}	$f_{0.7}$
22.5 – 23.5	data	0.46	0.13
	UL ^a	≤ 0.48	≤ 0.24
	PLE	0.50	0.27
	G95 ^b	0.76-1.31	0.55-0.82
22.5 – 24	data	0.46	0.12
	UL	≤ 0.56	≤ 0.38
	PLE	0.59	0.40
	G95	0.83-1.39	0.61-0.84

^a Upper limits if z -unidentified galaxies are at $z > 0.7$

^b PLE models by Glazebrook et al. (1995)

tions of the $\Omega = 0$ reference PLE model. The model can be reconciled with the data only if all, or at least most of the galaxies without measured z in the indicated magnitude range are at high z . This assumption will be discussed in §3.6. Our PLE model is in good agreement with the spectroscopic data of the two B -selected SSA13 and SSA22 Hawaii Survey fields (Cowie, Hu & Songaila 1995): all 9 galaxies with $B \leq 23$ have $z \leq 0.7$, and for $23 < B \leq 24$, 8 galaxies out of 21 (38%) with measured z have $z > 0.7$.

The nE model distribution is in good agreement with the data in the four panels of Fig 10. The nE model requires

the z distribution of the z -unidentified galaxies not to be very different from that of the galaxies with measured z . However, it is important to recall here the failure of the nE model to reproduce the counts and the colour distributions at faint magnitude (§3.3.1).

Note that we have not included in our models the $(1+z)^4$ dependence of the surface brightness with z , which decreases the fraction of expected high z galaxies (Yoshii & Peterson 1995). The magnitude of this effect is a function not only of the intrinsic parameters of the galaxies, but also of the details of the data reduction procedure adopted in the construction of the photometric catalogs from which the galaxies to be observed spectroscopically are selected. Other effects, such as dust extinction inside galaxies (GK95), which have not been considered in our models can decrease the predicted number of high z galaxies.

To compare different PLE models, we list in Table 6 the range of z_{med} and $f_{0.7}$ computed by Glazebrook et al. (1995a) from their PLE models. The Glazebrook et al. values are significantly higher than ours. The same is true for the GRV90 and Metcalfe et al. (1995a) PLE models. The basic reasons for this difference are the milder galaxy evolution assumed in our PLE models, and/or the more crude treatment of luminosity and spectral evolution of galaxies in the quoted papers. For example, in the Glazebrook et al. (1995a) model, a single SFR history is adopted for all morphological types. On the other hand, the KGB93 and GK95 models produce values of z_{med} and $f_{0.7}$ slightly lower than ours and, therefore, in good agreement with the data. However, the KGB93 model also predicts a significant population of low luminosity galaxies at $z < 0.2$, which is not seen in the Glazebrook et al. data.

3.5.2 I and K bands

In Fig 11 we compare the z distribution derived from the large and deep z surveys of Crampton et al. (1995, I -selected) and Songaila et al. (1994, K -selected) with the models. The z distribution in panel (a) is characterized by $\langle z \rangle = 0.56$, $z_{med} = 0.57$, and $f_{0.7} = 0.34$. The $\Omega = 0$ reference PLE model predicts $\langle z \rangle = 0.58$, $z_{med} = 0.54$, and $f_{0.7} = 0.30$, in excellent agreement with the data. The high z E/S0 galaxies predicted at $b_j \gtrsim 23.5$ have a mean $\langle b_j - I \rangle < 1$, corresponding to $\langle I \rangle \gtrsim 22.5$, and are, therefore, not expected in significant numbers in this survey limited at $I = 22.0$. The nE model z distribution, $\langle z \rangle = 0.48$, $z_{med} = 0.47$, and $f_{0.7} = 0.18$, does not reproduce well the tail of high z galaxies observed in this survey. The I band LF derived from the Crampton et al. (1995) data set (see Fig 6 of Lilly et al. 1995b), as well as the E galaxy LF constructed from the HST Medium Deep Survey (estimating z photometrically, Im et al. 1995), show clear evidence of evolution for $z \leq 1$. The amount of evolution is consistent with the prediction of our PLE model: $\Delta I_z \sim -1.2$ up to $z = 1$.

To compare the models with the Songaila et al. (1994) z distribution, we have taken into account the decreasing area vs. increasing limiting K relationship of the survey as discussed in §3.4. The completeness of this spectroscopic survey is $\sim 100\%$ for $K < 18$ and $\sim 70\%$ for $18 < K < 20$. At variance with our z distribution for b_j -selected samples (Table 6), the $f_{0.7}$ upper limits derived from the K -selected data are significantly lower than the model values. For the

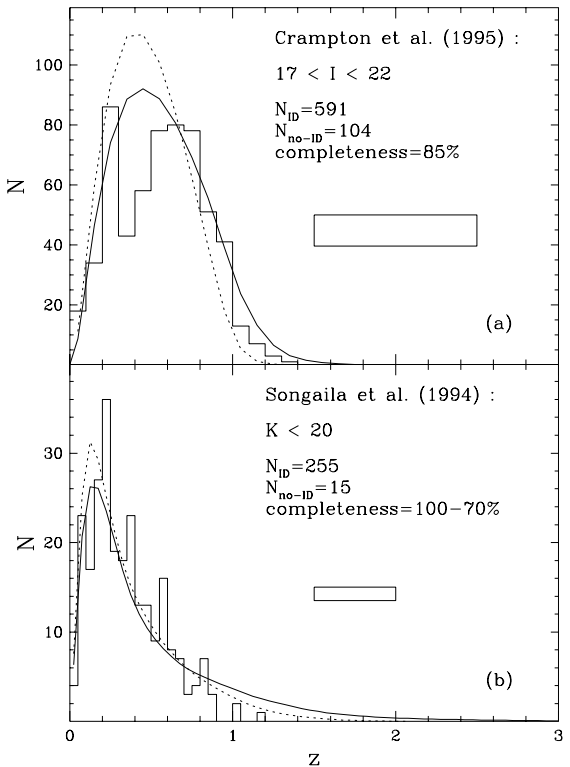


Figure 11. Redshift distributions for I and K selected samples. The source for the observed distributions (solid histogram) are indicated in each panel. The Crampton et al. (1995) data were kindly provided to us by L. Tresse. The two values for completeness of the Songaila et al. sample refer to $K < 18$ and $K > 18$, respectively. Dotted line: nE model; solid line: PLE model; both for $\Omega = 0$, $z_f = 4.5$.

observed z distribution in Fig 11, panel (b), $f_{0.7} = 0.08$. The PLE model predicts $f_{0.7} = 0.23$, well above the upper limit $f_{0.7} < 0.13$ derived assuming that all galaxies with no measured z have $z > 0.7$. This result indicates that there may be a problem in one or more of the ingredients or assumptions that go into our PLE models. The spectroscopic incompleteness of the sample is important at the faint level, but it cannot be the only cause of the problem since the discrepancy is already present in the bin $17 < K < 18$, where the spectroscopic survey is complete. In this bin, the upper limit from the observed distribution is $f_{0.7} < 0.16$, and the model predicts $f_{0.7} = 0.37$. We think that the evolutionary rate in the K band has to be revised in order to explain the observations. We are currently exploring galaxy evolution models based on different sets of evolutionary tracks and stellar spectral libraries (Bruzual 1995) to evaluate their effect on PLE models.

3.6 On the nature of z -unidentified galaxies

Since most z surveys are based on spectra which cover the range from ~ 3700 to ~ 7500 Å, the [OII] $\lambda 3727$ line (most prominent feature in low S/N galaxy spectra) can be used as a z indicator only up to $z \sim 1$. Higher z galaxies are difficult to identify because of the lack of features in the UV

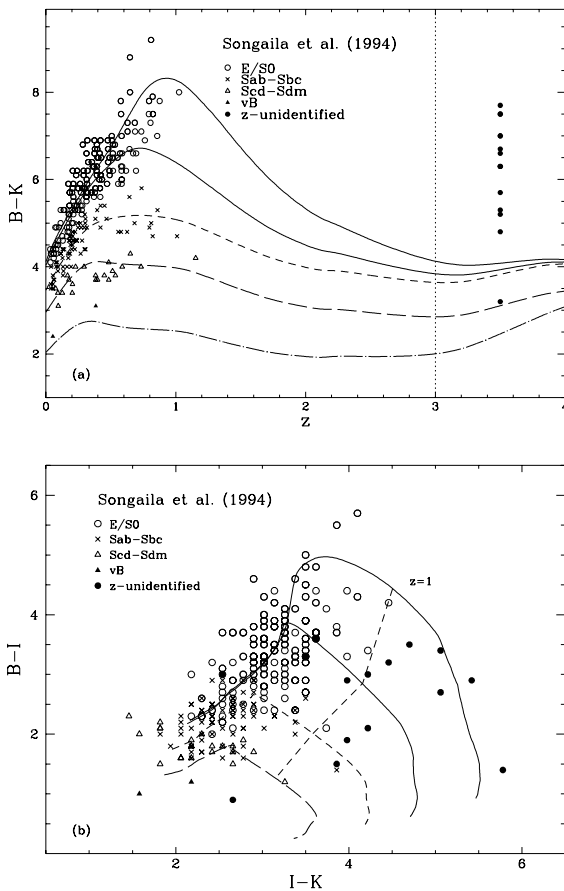


Figure 12. (a) $B - K$ colour as a function of z for the Songaila et al. sample. The solid dots correspond to the z -unidentified galaxies in the survey and are plotted arbitrarily at $z = 3.5$. The lines represent the colour predicted for each morphological type by the BC93 models listed in Table 3 for the $\Omega = 0$ reference model. E/S0: solid lines; Sab-Sbc: short-dashed line; Scd-Sdm: long-dashed line; vB: dot-dashed line. (b) $B - I$ vs. $I - K$ for the same sample. The lines have the same meaning as in (a). The $z = 1$ locus is indicated. See text for details.

rest frame spectra of typical galaxies. This fact, by itself, suggests the possibility that a large fraction of the galaxies with no measured z is at high z . This assumption is also supported by an analysis of the colour distributions of these galaxies. We discuss here in detail the behavior of the $B - I$ and $I - K$ colours in the Songaila et al. (1994) sample. Fig 12a shows $B - K$ vs. z for all galaxies in the sample, discriminated by morphological type accordingly to the closest proximity of the galaxy colour to the BC93 model colour for the class at the same z . Most of the z -unidentified galaxies (black dots in the plot) are consistent with the model colours of E/S0s at $z > 0.2$. In Fig 12b the same galaxies are plotted in the $B - I$ vs. $I - K$ plane. The lines show the expected location of galaxies of different morphological type at increasing z . Two things are interesting to note: first, galaxies of all types fall reasonably well in the appropriate region in this plane. Second, a large fraction of the z -unidentified galaxies has colours consistent with being early-type galaxies at $z > 1.0$. We have verified *a posteriori* the reliability of the photometric z estimates by examining the measured z of galaxies with colours close to the expected colour at $z = 1$:

7 out of 8 such galaxies have $0.64 < z < 1.16$. Thus, it seems reasonable to assume that most of the z -unidentified galaxies in this sample are actually at high z .

This conclusion is consistent with the Keck telescope spectroscopic observations of faint galaxies ($K < 20, I < 22.5, B < 24.5$) by Cowie et al. (1995b). Their data show strong evidence of a significant fraction of high- z luminous star forming galaxies. Of 333 galaxies that have been observed, z could be measured for 281 galaxies. 91 galaxies ($\sim 32\%$) have $z > 0.7$ and 40 galaxies ($\sim 14\%$) have $z > 1$. Cowie et al. argue that inspection of the $B - I$ vs. $I - K$ colour-colour plane suggests that most of the remaining unidentified objects are luminous high z star forming galaxies.

The same type of analysis cannot be applied to the b_j -selected survey of Glazebrook et al. (1995a) because only $B - R$ is available for these galaxies. The photometric z estimates using a single colour are less accurate. The $B - R$ distribution suggests a higher percentage of late type galaxies in this sample than in the K -selected sample, in agreement with our model for the number counts (§3.3.4).

4 CONCLUSIONS

The detailed comparison of a large amount of faint galaxy survey data and the predictions of new models has provided the following results.

(i) The $\Omega = 0$ nE model fits reasonably well the observed (U, b_j, r_f, I) counts up to $\sim (21, 22, 22, 23)$, respectively. At fainter magnitude the counts show an excess with respect to the nE model in all bands, except in K . The excess in the b_j counts amounts to $N_{obs}/N_{nE} \sim 3$ at $b_j \sim 26$, and is lower than in previous studies by a factor of ~ 2 . This difference is due to our choice of normalizing the model counts to the observed number in the range $19.0 < b_j < 19.5$, and to the higher UV flux in the BC93 models of local E/S0's than in the SEDs used in previous nE models (GRV90, Maddox et al. 1990).

(ii) A PLE model, in which galaxies are characterized by the LF and SEDs listed in Table 1 and Table 3 for the ($\Omega = 0, z_f = 4.5, t_g = 16$ Gyr) Friedmann cosmology, provides good fits to most of the existing data from faint galaxy surveys. In particular, it reproduces well the faint galaxy counts in the U, b_j, r_f, I and K bands, as well as the colour distributions of blue and K -selected samples up to the faintest observational limits, and the z distributions of b_j -, I - and K -selected samples up to $b_j < 23, I < 22$, and $K < 17$. In the magnitude range $23 \leq b_j \leq 24$, the predictions from the model can still be reconciled with the data if most of the galaxies without a z determination are at relatively high z ($z > 0.7$).

(iii) The steep slope of the APM counts at bright b_j requires strong evolution even at relatively small z (Maddox et al. 1990). This is in conflict with the mild amount of evolution required to fit the z and colour distributions at fainter magnitude. It has been suggested that the low counts at bright magnitude may be produced by either photometric errors (Metcalfe et al. 1995b) and/or by the fact that photographic surveys may have missed a significant population of low surface brightness galaxies because of the relatively high isophotal limits in these surveys (McGaugh 1994; Ferguson & McGaugh 1995).

(iv) PLE models in a flat $\Omega = 1$ universe cannot reproduce several aspects of the data. In particular, the faint counts are significantly below the observed ones in all bands, including K . A NLE model in an $\Omega = 1$ universe, in which galaxy density increases as $(1+z)^2$ due to merger events is found to reproduce satisfactorily the counts (see also RVG90). However, we consider that a more realistic model, which takes into account the change of the galaxy photometric properties when the merging occurs, must be explored before this result can be taken at face value.

(v) The Scalo IMF, being relatively poor in massive stars, produces models for early-type galaxies which are considerably less luminous in the UV at early epochs than the Salpeter IMF models. This lower flux translates into a milder spectral evolution, as required by the observed z distributions of faint galaxies. Scalo IMF models are thus preferred for early-type galaxies over Salpeter IMF models.

(vi) The observed $b_j - r_f$ and $B - K$ colour distributions are reproduced more closely by our PLE models if we assume that star formation in E/S0 galaxies extends over a longer period of time (τ_1 and τ_2 models) than in a short box-type burst models (B_1 model).

(vii) At faint magnitude ($b_j \gtrsim 23, K \gtrsim 18$) our PLE model predicts a significant fraction of high- z galaxies, mostly blue young early-type E/S0 and Sab-Sbc galaxies. The predictions of this model are in excellent agreement with the $B - K$ colours of the Hawaii K -selected survey which failed to reveal galaxies at high z with colours as red as those of local E/S0 galaxies (Gardner 1995). On the other hand, recent results on the LF of red and blue galaxies in the CFRS sample suggest evolution of the blue galaxies and not of the red galaxies (Lilly et al. 1995b). This appears to be in contradiction with our model and to favor models in which a significant amount of the luminosity evolution needed to fit the faint counts is due to spiral rather than early-type galaxies. A discussion of these models can be found in Campos & Shanks (1995).

(viii) The most significant remaining discrepancy between our PLE model and the data is in the z distribution of the Songaila et al. (1994) K -selected sample at $K > 17$. The fraction of galaxies at high z predicted by the model is significantly higher, by a factor of $\sim 2 - 3$, than observed. The discrepancy persists even if, as suggested by their colours, most of the galaxies which have been observed spectroscopically and for which no z could be measured, are at high z . Thus, on the one hand, the z distribution of these galaxies seems to rule out evolution. On the other hand, the K band LF (Glazebrook et al. 1995b) indicates that galaxies at $z = 1$ are ~ 0.75 magnitude brighter than local ones, consistent with PLE models. Only additional spectroscopy of faint K -selected galaxies can resolve this apparent contradiction between different data sets.

In summary, simple PLE models, together with an appropriate selection of galaxy evolution models (SFR and IMF) which provide mild luminosity evolution at least up to $z = 1$ in an $\Omega = 0$ universe, can still be considered as baseline models. Additional improvements should be considered in this framework, for example: (a) Introduction of different z_f for galaxies of different morphological type and/or different luminosity. This could help in explaining the colour-luminosity relation, observed in cluster galaxies

(see Bower, Lucey & Ellis 1992 for ellipticals and Gavazzi 1993 for both early and late types). (b) Spectrophotometric models which include chemical and dynamical evolution (Bressan, Chiosi & Fagotto 1994) predict that E/S0 galaxies approach their local colour at younger ages than in chemically homogeneous models. This faster rate of evolution might bring the predictions of the $\Omega = 1$ PLE model in better agreement with the observations and should be explored in detail. (c) Introduction in the models of at least the most important observational selection effects, e.g. the surface brightness selection (McGaugh 1994, Yoshii & Peterson 1995). (d) A detailed analysis of the effects of extinction by dust (GK95, Campos & Shanks 1995), taking into account the time evolution of the amount of dust inside galaxies, which can be particularly important at high z .

The interested reader may request the k - and $(e + k)$ -corrections required to reproduce these models via e-mail from G.B.A. or L.P.

ACKNOWLEDGMENTS

G.B.A. was supported by SFB 328 during his visit to the Landessternwarte Heidelberg Königstuhl. L.P. acknowledges the hospitality of the Landessternwarte Heidelberg Königstuhl and the Centro de Investigaciones de Astronomía during the realization of this project, as well as the support of the EEC program No. CHRX-CT92-0033. We thank an anonymous referee for his/her careful reading of the first version of this paper, and for challenging us to make this paper shorter and more interesting. We expect to have succeeded.

REFERENCES

Babul A., Rees M.J., 1992, MNRAS, 255, 346
 Bingelli B., Sandage A., Tamman G.A., 1988, ARA&A, 26, 509
 Bower R.G., Lucey J.R. & Ellis R.S., 1992, MNRAS, 254, 589
 Bressan A., Chiosi C., Fagotto F. 1994, ApJS, 94, 63
 Broadhurst T.J., Ellis R.S., Shanks T., 1988, MNRAS, 235, 827
 Broadhurst T.J., Ellis R.S., Glazebrook K., 1992, Nat, 355, 55
 Bruzual A., G., 1995, in From Stars to Galaxies, eds. C. Leitherer, U. Fritze-v.Alvensleben and J. Huchra, PASP Conference Series, in press.
 Bruzual A., G., Charlot S., 1993, ApJ, 405, 538 (BC93)
 Bruzual A., G., Kron R.G., 1980, ApJ, 241, 25 (BK80)
 Buser R., 1978, A&A, 62, 411
 Campos A., Shanks T., 1995, Durham astro-ph/9511110
 23-Nov-95 preprint
 Carlberg R.G. & Charlot S., 1992, ApJ, 397, 5
 Colless M., Ellis R.S., Taylor K., Hook R.N., 1990, MNRAS, 244, 408
 Colless M., Ellis R.S., Broadhurst T.J., Taylor K. & Peterson B.A., 1993, MNRAS, 261, 19
 Colless M., 1995, in Maddox S.J. & Aragón-Salamanca A., eds, Wide Field Spectroscopy and the Distant Universe, World Scientific, p. 263
 Couch W.J., Newell E.B., 1980, PASP, 92, 746
 Cowie L.L., Songaila A., Hu E.M., 1991, Nat, 354, 460
 Cowie L.L., Gardner J.P., Hu E.M., Songaila A., Hodapp K.-W. and R.J. Wainscoat R.J., 1994, ApJ, 434, 114
 Cowie L.L., Hu E.M., & Songaila A., 1995a, AJ, 110, 1576
 Cowie L.L., Hu E.M., & Songaila A., 1995b, Nat, 377, 603
 Crampton D., Le Fèvre O., Lilly S.J., Hammer F., 1995, ApJ, 455, 96 (CFRS V)
 Djorgovski S., Soifer B.T., Pahre M.A., Larkin J.E., Smith J.D., Neugebauer G., Smail I., Matthews K., Hogg D.W.,

Blandford R.D., Cohen J., Harrison W., Nelson J., 1995, *ApJ*, 438, L13

Efstathiou G., Ellis R.S., Peterson B.A., 1988, *MNRAS*, 232, 431

Ellis R.S., 1983, in Jones B.J.T., Jones J.E., eds, *The Origin and Evolution of Galaxies*. Reidel, Dordrecht, p. 255

Ellis R.S., Colless M., Broadhurst T., Heyl J., Glazebrook K., *astro-ph/9512057* 11-Dec-95 preprint

Ferguson H.C. & McGaugh S.S., 1995, *ApJ*, 440, 470

Fritze-v. Alvensleben, U. & Gerhard, O.E., 1994, *A&A*, 285, 751

Fukugita M., Takahara F., Yamashita K., Yoshii Y., 1990, *ApJ*, 361, L1

Gardner J.P., 1995, *ApJ*, 452, 538

Gardner J.P., Cowie L.L., Wainscoat R.J., 1993, *ApJ*, 415, L9

Gavazzi G., 1993, *ApJ*, 419, 469

Glazebrook K., Peacock J.A., Collins C.A. & Miller L., 1994, *MNRAS*, 266, 65

Glazebrook K., Ellis R., Colless M., Broadhurst T., Allington-Smith J. and Tanvir N., 1995a, *MNRAS*, 273, 157

Glazebrook K., Peacock J.A., Miller L., Collins C.A., 1995b, *MNRAS*, 275, 169

Guiderdoni B., Rocca-Volmerange B., 1987, *A&A*, 186, 1 (GRV87)

Guiderdoni B., Rocca-Volmerange B., 1990, *A&A*, 227, 362 (GRV90)

Guiderdoni B., Rocca-Volmerange B., 1991, *A&A*, 252, 435 (GRV91)

Gronwall C., Koo D.C., 1995, *ApJ*, 440, L1 (GK95)

Hall P., Mackay C.B., 1984, *MNRAS*, 210, 979

Hammer F., Crampton D., Le Fèvre O., Lilly S.J., 1995, *ApJ*, 455, 88 (CFRS IV)

Infante L., Pritchett C., Quintana H., 1986, *AJ*, 91, 217

Im et al. 1995, in preparation

Jones L.R., Fong R., Shanks T., Ellis R.S., Peterson B.A., 1991, *MNRAS*, 249, 481

King C.R. & Ellis R.S., 1984, *ApJ*, 288, 456

Koo D.C., 1981, Ph.D. thesis, University of California, Berkeley

Koo D.C., 1985, *AJ*, 90, 418

Koo D.C., 1986, *ApJ*, 311, 651

Koo D.C., Gronwall C., Bruzual A., G., 1993, *ApJ*, 415, L21 (KGB93)

Koo D.C., Kron R.G., 1992, *ARA&A*, 30, 613

Kron R.G., 1980, *ApJS*, 43, 305

Le Fèvre O., Crampton D., Lilly S.J., Hammer F., Tresse L., 1995, *ApJ*, 455, 60 (CFRS II)

Lilly S.J., Cowie L.L. & Gardner J.P., 1991, *ApJ*, 369, 79

Lilly S.J., 1993, *ApJ*, 411, 501

Lilly S.J., Hammer F., Le Fèvre O., Crampton D., 1995a, *ApJ*, 455, 75 (CFRS III)

Lilly S.J., Tresse L., Hammer F., Crampton D., Le Fèvre O., 1995b, *ApJ*, 455, 108 (CFRS VI)

Loveday J., Peterson B.A., Efstathiou G., Maddox S.J., 1992, *ApJ*, 390, 338

Madau P., 1995, *ApJ*, 441, 18

Maddox S.J., Sutherland W.J., Efstathiou G., Loveday J., and Peterson B.A., 1990, *MNRAS*, 247, *Short Comm.*, 1p

Magris G.C. & Bruzual A., G., 1993, *ApJ*, 417, 102

Majewski S.R., 1989, in Frenk C.S. et al., eds, *The Epoch of Galaxy Formation*. Kluwer, Dordrecht, p. 85

McGaugh S., 1994, *Nat*, 367, 538

McLeod B.A., Bernstein G.M., Rieke M.J., Tollestrup E.V., Fazio G.G., 1995, *ApJS*, 96, 117

Metcalfe N., Shanks T., Fong R., Jones L.R., 1991, *MNRAS*, 249, 498

Metcalfe N., Shanks T., Fong R., Roche N., 1995a, *MNRAS*, 273, 257

Metcalfe N., Fong R., Shanks T., 1995b, *MNRAS*, 274, 769

Mobasher B., Ellis R.S., Sharples R.M., 1986, *MNRAS*, 223, 11

Mobasher B., Sharples R.M., Ellis R.S., 1995, *MNRAS*, 263, 560

Pence W., 1976, *ApJ*, 203, 39

Fong R. & ZenLong Z., 1986, *MNRAS*, 221, 233

Picard A., 1991, *AJ*, 102, 445

Rocca-Volmerange B., Guiderdoni B., 1988, *A&AS*, 75, 93

Rocca-Volmerange B., Guiderdoni B., 1990, *MNRAS* 247, 166 (RVG90)

Salpeter E.E., 1955, *ApJ*, 121, 161

Scalo J.M., 1986, *Fund Cosmic Phys*, 11, 1

Schechter P., 1976, *ApJ*, 203, 297

Shanks T., 1990, in Bowyer S., Leinert Ch., eds, *Galactic and Extragalactic Background Radiation: Optical, Ultraviolet, and Infrared Components*, IAU Symp. 139. Kluwer, Dordrecht, p. 269

Shanks T., Stevenson P.R.F., Fong R., MacGillivray H.T., 1984, *MNRAS*, 206, 767

Soifer B.T., Matthews K., Djorgovski S., Larkin J., Graham J.R., Harrison W., Jernigan G., Lin S., Nelson J., Neugebauer G., Smith G., Smith J.D., and Ziolkowski C., 1994, *ApJ*, 420, L1

Songaila A., Cowie L.L., Hu E.M., Gardner J.P., 1994, *ApJS*, 94, 461

Steidel C.G., Hamilton D., 1993, *AJ*, 105, 2017

Stevenson P.R.F., Shanks T., Fong R., 1986, in Chiosi C. & Renzini A., eds, *Spectral Evolution of Galaxies*. Reidel, Dordrecht, p. 439

Tinsley B.M., 1980, *ApJ*, 241, 41

Tresse L., Hammer F., Le Fevre O., and Proust D., 1993, *A&A*, 277, 53

Tyson J.A., 1984, in Capaccioli M., eds, *Astronomy with Schmidt-Type Telescopes*. Reidel, Dordrecht, p. 489

Tyson J.A., 1988, *AJ*, 96, 1

Yee H.K.C., Green R.F., 1987, *ApJ*, 319, 28

Yoshii Y. & Peterson B.A., 1995, *ApJ*, 444, 15

Wainscoat R.J., Cowie L.L., 1992, *AJ*, 103, 332

Weir N., 1994, Ph.D. thesis, California Institute of Technology

Peacock J.A., eds, *The Epoch of Galaxy Formation*. Kluwer, Dordrecht, p. 15

Zucca E., Pozzetti L., Zamorani G., 1994, *MNRAS* 269, 953

Zwicky F., Herzhog E., Wild P., Karpowicz M., Kowal C.T., 1961-1968, *Catalogue of Galaxies and Cluster of Galaxies*, California Institute of technology, Pasadena

This paper has been produced using the Blackwell Scientific Publications *T_EX* macros.

